Green Energy and Sustainability
https://doi.org/10.47248/ges2606010001

Original Research

Preliminary analysis of components cost distribution for a low enthalpy geothermal power plant

Antonios Iasonas Karypidis [1], Dimitrios Misirlis [1,*], Christiana Papapostolou [2], Kostas Kleidis [1]

1. Department of Mechanical Engineering, International Hellenic University, Terma Magnesias, 62124, Serres, Greece; Emails: tonyiaso@hotmail.com (A.I.K.); kleidis@ihu.gr (K.K.)
2. Department of Mechanical Engineering, University of West Attica, Ancient Olive Grove Campus, 250 Thivon & P. Ralli Str, Egaleo, 12241, Athens, Greece; Email: chrispap@uniwa.gr

* **Correspondence:** Dimitrios Misirlis; Email dmissirlis@ihu.gr

Cite This Article:
Karypidis AI, Misirlis D, Papapostolou C, Kleidis K. Preliminary analysis of components cost distribution for a low enthalpy geothermal power plant. Green Energy Sustain. 2026;6(1):0001. https://doi.org/10.47248/ges2606010001

Received: 27 Sep 2025
Accepted: 8 Dec 2025
Published: 9 Jan 2026

Copyright:
© 2026 by the author(s). This is an Open Access article distributed under the Creative Commons License Attribution 4.0 International (CC BY 4.0) license, which permits unrestricted use, distribution and reproduction in any medium or format, provided the original work is correctly credited.

Publisher's Note:
Pivot Science Publications remains neutral with regard to jurisdictional claims in published maps and institutional affiliations.

Abstract

In the present work, a focused analysis of the cost-components distribution of a low-enthalpy Rankine cycle using supercritical carbon dioxide (sCO_2) as the working fluid is made. This investigation aims to evaluate the cost distribution of the main sCO_2 components and identify the most cost-intensive elements to support future techno-economic assessments of low-enthalpy power plants. More specifically, the present work explores the utilization of a low-enthalpy geothermal field located in the Sidirokastro area, in Serres region in Greece, for approximately 250 kW of power generation, with a maximum geothermal water source temperature of 78 °C. To estimate the thermodynamic performance of this specific geothermal field, a thermodynamic model was developed, modelling a transcritical Rankine cycle using sCO_2 as the working fluid. The thermodynamic model was developed using the Cape Open to Cape Open (COCO) simulator and incorporated the most recent available data describing the geothermal source properties and typical performance characteristics of the main thermodynamic cycle components. Furthermore, the Peng-Robinson equation of state was used, to estimate the thermophysical properties of sCO_2. For the calculation of the low-enthalpy power plant, a preliminary assessment of the purchase cost of the main components of the geothermal power plant was performed, based on the most updated correlations from international literature. These correlations connect the equipment purchase cost to the key operational parameters, such as the power output and the UA value (the product of the overall heat transfer coefficient and the heat exchanger surface area). To improve the accuracy of the calculation of the UA parameter in the power plant heat exchangers, detailed sub-models for the geothermal heat exchanger and the water condenser were used. These models allow to properly capture the effect of the CO_2 thermophysical properties variations to the calculation of the logarithmic mean temperature difference and thus, to the UA parameter value. The analysis of the results led to the identification of the most important components of the geothermal power plant from a cost-intensive point of view. More specifically, the condenser and the geothermal heat exchanger, accounted for over 55% of the total cost, with the water condenser cost corresponding to 32.44% and the one of the geothermal heat exchanger to 23.05%. These findings provide valuable insights for future techno-economic analyses aiming at the evaluation and optimization of the performance of low-enthalpy geothermal power plants.

Keywords: Low enthalpy geothermal plant; heat exchangers; component cost; cost function

1. Introduction

Nowadays, various research activities and policy initiatives are being undertaken towards the achievement of climate neutrality and zero greenhouse gases emissions by 2050. One of the most significant of these initiatives is the European Grean Deal [1]. The achievement of the targets set by the European Green Deal requires the maximization of renewable energy sources utilization. In this context, geothermal energy can play a pivotal role, as it is a clean energy source that appears to have the highest technological potential compared to other renewable energy sources [2] since it is renewable, environmentally friendly, and has an exceptional availability (capacity factor >90%) [3].

In terms of availability, only a relatively small percentage of geothermal fields, e.g., ~10–15% in Southern Europe, have temperatures exceeding 80 °C. Conversely, a vast geothermal potential can be found in low-enthalpy geothermal fields (at a maximum temperature in the range of 60-75 °C), which remains mostly unexploited despite being typically located at shallow depths where drilling costs are considerably lower. This is due to a number of complex factors, including limited regulatory and market support frameworks and the prioritization of other renewable energy sources such as wind and solar power. These low-enthalpy geothermal fields account for almost ~40% of the total geothermal supply in Southeast Europe [4]; consequently, their utilization for power generation represents an attractive opportunity. Efforts for electricity power generation from low-enthalpy geothermal fields have previously been reported in countries such as USA (Chena, Alaska, 400 kW), Mexico, the Philippines, Indonesia, Austria, Germany, Turkey (Atca Project, Denizli, 32.8 MW) and Iceland [2,5,6]. However, in most developing countries, low enthalpy geothermal power generation has not yet received significant attention for electricity production, as there are concerns about its economic viability for commercial- scale electricity generation [2,5].

Recent geostrategic developments along with the resulting rising energy costs and uncertainty over future energy supplies, have improved the attractiveness of low-enthalpy geothermal energy resources, which can be exploited for electricity generation using binary cycles [7–9]. For the utilization of low-enthalpy geothermal fields, binary cycle power plants represent the most promising option, as they have the capability to exploit lower-temperature level sources and binary thermodynamic cycles [4]. This technology has virtually no greenhouse gas emissions (GHG) into the atmosphere [2,5,7] and is also promising due to its simplicity and relatively limited number of components/parts, most of which are commercially available. As a result, binary cycles power plants are the fastest-growing category of geothermal energy utilization systems [10].

However, to sustainably meet future energy requirements, the use of geothermal energy must be both technically and economically viable. Thus, the effective utilization of low-enthalpy geothermal energy requires careful consideration of cost-related economic factors [11]. Various factors affect the performance of binary-cycle power plants: the temperature level of the external source, the working fluid, the type of turbine, the condensation temperature, and the operating conditions in general. Therefore, the configuration of a typical binary-cycle power plant varies significantly, depending on the specific application, and no standard design has been established [12–14] as the absolute optimum.

The first low-enthalpy binary-cycle power plants were constructed in 1952, in the Democratic Republic of Congo, 200 kW (geothermal water temperature 91 °C) and in 1967 in Kamchatka in the USSR, (670 kW, geothermal water temperature 85 °C) [13]. These plants demonstrated that it is possible to generate electricity profitably if the condensation temperature of the working fluid is kept sufficiently low, as evidenced by the case of the plant in Chena, Alaska (210 kW, geothermal water temperature ~74 °C, average condensation temperature ~5 °C) [15] and the case of the LOW-BIN project, "Efficient Low Temperature Geothermal Binary Power" [6,16].

Greece is particularly rich in low-enthalpy geothermal fields and has a long experience in geothermal energy utilization, mainly for medical and therapeutic purposes. However, until now the use of geothermal energy for electricity generation has not been possible, with the only noteworthy effort being the 2 MW geothermoelectric pilot plant that operated in Milos for only ten months in the late 1980s. This plant, which utilized a high enthalpy field, was not fully accepted by the local community, mainly due to a lack of awareness concerning the environmental and economic advantages of geothermal energy. On the other hand, despite the existence of many low-enthalpy geothermal fields, in other Greek areas (e.g., Lesvos, Evros and Sidirokastro), these are currently used almost exclusively for greenhouses' heating purposes [17,18]. The growing demand for clean, efficient, and renewable energy sources renders low-enthalpy geothermal energy exploitation as one of the most promising sectors in the future energy mix, particularly due to its abundance in countries such as Greece. In this context, binary-cycle power plants, typically based on organic Rankine cycles (ORC), have emerged as a particularly effective technological solution for electricity generation from medium and/or low-temperature geothermal fields, which are widespread in Greece. Unlike the classical Rankine cycle that uses water as the working fluid, the organic cycle uses organic fluids (e.g., R134a) with a lower boiling point. This allows for efficient conversion of thermal energy into electrical energy even when the available temperatures are below 150 °C. This makes ORC technology ideal for exploiting low and medium enthalpy geothermal resources.

In a binary cycle ORC power plant, the selection of an appropriate working fluid can be of critical importance especially when environmental parameters such as GWP- Global Warming Potential or ODP - Ozone Depletion Potential are considered. Working fluids such as R134a, R236ea, R245fa, and R142b are suitable for low enthalpy applications in the temperature range of 50-100 °C [19]. However, when more strict environmental concerns are considered the use of these fluids can become potentially problematic, since their GWP and ODP values are usually relatively high or present safety level concerns. In addition, taking into account the planned hydrofluorocarbon (HFC) phase-down in Europe in 2030 [20], due to the fact that HFCs may account as responsible for the majority of fluorinated greenhouse gases emissions, the substitution of HFCs with cleaner, environmentally friendlier, and non-toxic working fluids has become increasingly important. Consequently, the use of less conventional fluids such as carbon dioxide, with a GWP of 1 and an ODP of 0, is gaining attention, making the quantification of their thermodynamic performance and component costs highly relevant.

Such an effort is undertaken in the current work which investigates the thermodynamic performance and the components cost of a low-enthalpy geothermal binary-cycle power plant using supercritical carbon dioxide as its working fluid. Supercritical carbon dioxide binary-cycles gained substantial attention during the past decade due to their potential for achieving higher thermodynamic efficiency compared to conventional steam-based Rankine cycles. The low-enthalpy geothermal field under investigation is located in Sidirokastro region (Serres area, Greece), shown in **Figure 1**, where recent studies conducted by the Hellenic Authority for Geological and Mineral Research identified a geothermal fluid reservoir with a maximum temperature of 78 °C at a depth of over 98 meters, with flow rates exceeding 120 m^3/h [21].

Figure 1. The Sidirokastro region in Serres and the estimated location of the low-enthalpy geothermal field (indicated by the blue dot, source: Google Earth).

2. Materials and Methods

2.1. Thermodynamic cycle model

The present work is investigating the utilization of a low-enthalpy geothermal field in the Sidirokastro area for the generation of approximately 250 kW of electrical power. Initially, to estimate the thermodynamic performance of this specific geothermal field, a numerical thermodynamic model was developed, modelling a transcritical Rankine cycle using sCO_2 as the working fluid.

The use of sCO_2 as the working fluid in a binary geothermal power plant based on a transcritical Rankine cycle has many advantages due to its unique properties. More specifically, carbon dioxide is an environmentally friendly, pollution free, non-flammable and widely available working fluid, which is also characterized by low-cost, low toxicity and low corrosivity. Furthermore, sCO_2 is a high-density working fluid enabling the use of highly compact turbomachinery components and heat exchangers. Supercritical CO_2 has also very good heat transfer properties (density, viscosity, thermal conductivity, heat capacity) and critical temperature similar to ambient conditions. Consequently, effective thermal matching can be achieved in the transcritical Rankine cycle during heat transfer processes. Finally, CO_2 has a GWP equal to 1 and an ODP equal to 0, values that provide significant environmental advantages in relation to other working fluids for similar applications (see **Table 1**).

Table 1. Properties of various working fluids (adapted data from [22-25]).

Fluid	Critical Temperature [°C]	Critical Pressure [Bar]	Safety Level	ODP	GWP
CO_2 (R744)	30.98	73.8	A1	0	1
Water (R718)	373.9	22.10	A1	0	0
R134a	101.1	40.7	A1	0	1430
R236ea	139.3	35.0	-	0	1410
R245fa	154.1	36.5	B1	0	1050
R142b	137.11	40.55	A2	0.06	2220
Ammonia (R717)	132.89	112.8	B2	0	0
Propane (R290)	96.7	42.47	A3	0	20
Butane (R600)	152	37.9	A3	0	20

The geothermal thermodynamic cycle examined in this study is a simple Rankine cycle comprising a geothermal water heat exchanger, an sCO_2 turbine, a condenser, and a pump, with sCO_2 used as the working fluid. The model was developed using the Cape Open to Cape Open (COCO) simulator [26] incorporating the most recent available data on geothermal source properties [27] and typical performance-characteristics of the main thermodynamic cycle components. The performance of the COCO simulator was validated in relation to commercial software, such as ASPEN, in various studies, e.g. in [28], showing close agreement. The geothermal power plant model is shown in **Figure 2**. The modelling equations and assumptions are presented in **Table 2**.

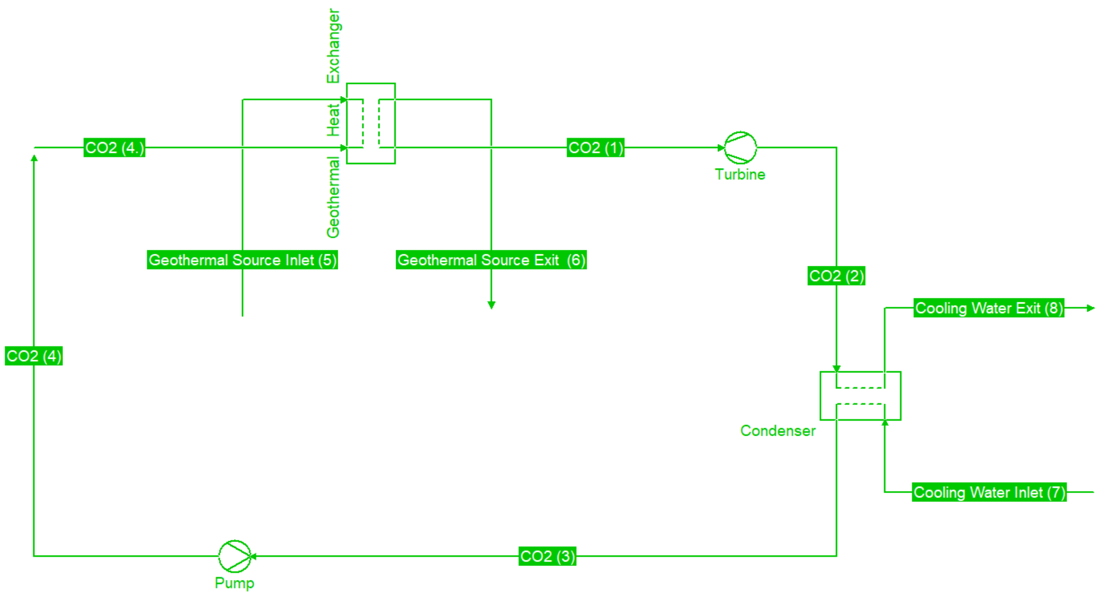

Figure 2. Geothermal power plant model developed in the COCO simulator.

Table 2. Thermodynamic equations and assumptions applied.

Components	Equations and assumptions
Geothermal heat exchanger (GHEX)	$\dot{Q}_{GHEX} = \dot{m}_{working\ fluid}(h_1 - h_4) = \dot{m}_{geothermal\ water}(h_5 - h_6)$
sCO_2 Turbine	$\dot{W}_t = \dot{m}_{working\ fluid}(h_1 - h_2)$
Condenser heat exchanger	$\dot{Q}_{cond} = \dot{m}_{working\ fluid}(h_2 - h_3) = \dot{m}_{cooling\ water}(h_8 - h_7)$
sCO_2 Pump	$\dot{W}_p = \dot{m}_{working\ fluid}(h_4 - h_3)$
Cooling water pump	$\dot{W}_{cw} = \dot{m}_{cooling\ water}(h_8 - h_7)$
Fluid mass flow rate	22.22 kg/s
Geothermal source maximum temperature	78 °C
Maximum pressure	100 bar
Condensation pressure	51.96 bar
Cooling water temperature	8 °C
Turbine isentropic efficiency	80%
Pump efficiency isentropic	80%
GHEX effectiveness	95%
Condenser effectiveness	95%
Geothermal water flow rate	120 m³/h

For the estimation of the sCO_2 thermophysical properties, the Peng-Robinson (1976) state-equation [29] was used based on the conclusions of the works of [30–32] where the Peng-Robinson state-equation was employed for modelling the sCO_2 thermophysical properties in ASPEN software.

$$P = \frac{RT}{V_m - b} - \frac{a\mathrm{a}}{V_m^2 + 2bV_m - b^2} \tag{1}$$

$$a = \frac{0.45724R^2T_c^2}{P_c} \tag{2}$$

$$b = \frac{0.07780RT_c}{P_c} \tag{3}$$

$$\mathrm{a} = \left(1 + (0.37464 + 1.54226\omega - 0.26992\omega^2)(1 - T_r^{0.5})\right)^2 \tag{4}$$

$$T_r = \frac{T}{T_c} \tag{5}$$

Concerning the geothermal plant thermodynamic model, it includes a geothermal heat exchanger where sCO_2 at 100bar pressure is heated by a low-enthalpy geothermal water source of maximum temperature of 78 °C. Then, the sCO_2 expands in the turbine, generating power and afterwards is condensed inside a condenser with the use of cooling water of 8 °C temperature and 4bar pressure. Finally, the sCO_2 exits the condenser in the form of liquid to properly feed and protect the pump, where the pressure is increased back at 100 bar. Regarding the selected operating characteristics of the cycle components, an isentropic efficiency of 80% was selected for both the sCO_2 turbine and the pump and an effectiveness of 95% for the geothermal heat exchanger and the water condenser heat exchanger.

2.2. Components cost model correlations

In the present study, a preliminary assessment of the purchase costs of the main geothermal power plant components was conducted based on dedicated correlations from international literature which relate the main power plant components to the key-operational characteristics, such as the power output and the UA parameter. These cost-correlations are mainly based on the works of Weiland et al. [33], Carlson et al. [34] and McCollum and Ogden [35]. Furthermore, where necessary, additional correlations from Towler and Sinnott

[36], Blecich and Blecich [37] and Shamoushaki et al. [38] were used. A summary of the adopted cost-components correlations is presented in **Table 3**.

Table 3. **Geothermal power plant cost-components correlations.**

Component	Component Cost Model	Scale Parameter	Reference
Geothermal Heat HEX	$49.45\cdot(UA)^{0.7544}$	UA [W/K]	Weiland et al. [33]
	$(-0.06395\cdot A^2+947.2P+\log A+227.9) * f_m * f_p$ f_m ...material correction factor and f_p ...pressure correction factor	Heat exchange area A [m^2]	Towler et al. [36] Blecich and Blecich [37]
Turbine	$406200\cdot(P^{0.8})$	Power [MW]	Weiland et al. [33]
Condenser	$C\cdot 49.45\cdot(UA)^{0.7544}$ C... material thickness correction term	UA [W/K]	Weiland et al. [33]
	$(-0.06395\cdot A^2+947.2P+\log A+227.9)\cdot f_m\cdot f_p$ f_m ...material correction factor and f_p ...pressure correction factor	Heat exchange area A [m^2]	Towler et al. [36] Blecich and Blecich [37]
Dry Cooler	$32.88\cdot(UA)^{0.75}$	UA [W/K]	Weiland et al. [33]
SCO_2 Pump	$(1.11\cdot 10^6)\cdot(P/1000) + 0.07\cdot 10^6$	Power [kW]	McCollum and Ogden [35]
	$(-0.03195\cdot P^2+467.2P+\log P+20480)\cdot f_m\cdot f_p$ f_m ...material correction factor and f_p ...pressure correction factor	Power [kW]	Towler et al. [36] Blecich and Blecich [37]
Pumps	$(-0.03195\cdot P^2+467.2P+\log P+20480)\cdot f_m\cdot f_p$ f_m ...material correction factor and f_p ...pressure correction factor	Power [kW]	Towler et al. [36] Blecich and Blecich [37]
Gearbox	$177200\cdot(P^{0.2434})$	Power [MW]	Weiland et al. [33]
Generator	$108900\cdot(P^{0.5463})$	Power [MW]	Weiland et al. [33]
Motors	$131400\cdot(P^{0.5611})$	Power [MW]	Weiland et al. [33]
Cooling Tower	$1500\cdot(V^{0.9}) +170000$	Volumetric flow rate [l/s]	Shamoushaki et al. [38] Blecich and Blecich [37]

To ensure the accuracy of the calculations of the UA parameter in the power plant's heat exchangers, detailed sub-models of the geothermal heat exchanger and the water-condenser heat exchanger were utilized, in which the overall heat transfer process in the heat exchangers was divided into various sub-units. At the next step, a sub-unit independency study was performed, considering the heat exchangers consisted of varying numbers of sub-units (1,5,10,15 and 20), in order to effectively capture the influence of the sCO_2 thermophysical property variations, mainly of enthalpy and specific heat capacity (C_p), on the calculation of the logarithmic mean temperature difference and thus, to the calculation of the overall UA parameter value in each heat exchanger. These sub-unit models were developed using the COCO simulator, applying four scenarios to both the geothermal water and cooling water condenser heat exchangers, with configurations of 5, 10, 15, and 20 sub-units, as illustrated in **Figure 3**. Then, the total UA value was calculated as the sum of the UA values of all sub-units of the heat exchangers.

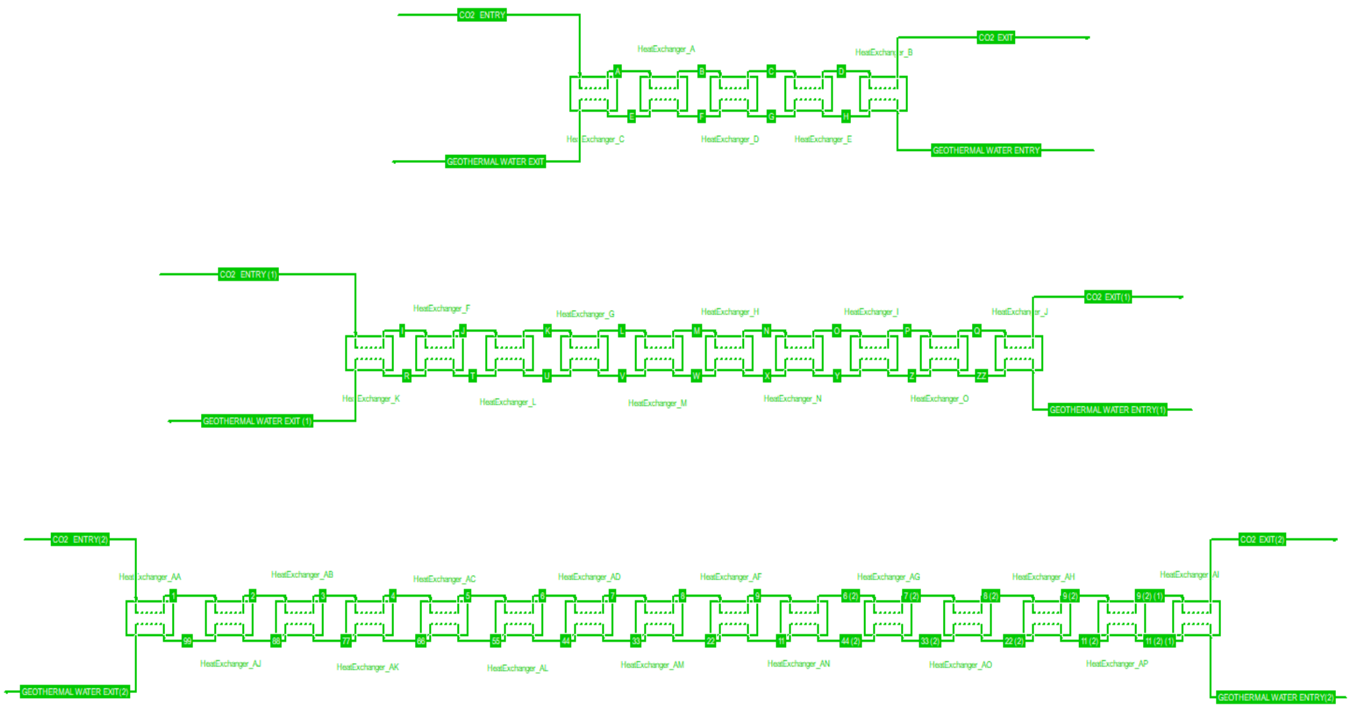

Figure 3. Indicative view of the heat exchanger sub-models for the 5, 10, 15 sub-units.

3. Results

In the next step a thermodynamic analysis of the binary-cycle power plant was conducted taking into account the thermodynamic conditions and components performance characteristics as described in **Table 2**. The selected operating conditions were determined based on the findings of the work of Karypidis et al. [27]. The main results of the binary cycle power plant are summarized in **Table 4**. The thermodynamic cycle of the binary plant under investigation is presented in **Figure 4**.

Table 4. Binary Cycle Main Results.

Component	Value	Unit
Geothermal Heat Exchanger	4586.15	kW
sCO_2 Turbine	425.33	kW
Condenser	4335.85	kW
Pump sCO_2	175.03	kW
Net Power	250.30	kW
Thermal efficiency	5.46	%

Furthermore, a sub-unit independency study using 1, 5, 10, 15 and 20 sub-units was performed for the geothermal heat exchanger and the condenser. The aim was to accurately estimate the total UA value for each heat exchanger of the geothermal power plant, as illustrated in **Figure 5** and **Figure 6**, by taking into proper consideration the thermophysical properties variation inside the heat exchangers during the heat transfer process. As one may observe, the total UA values are almost constant after the use of 15 sub-units in order to describe the heat exchange process.

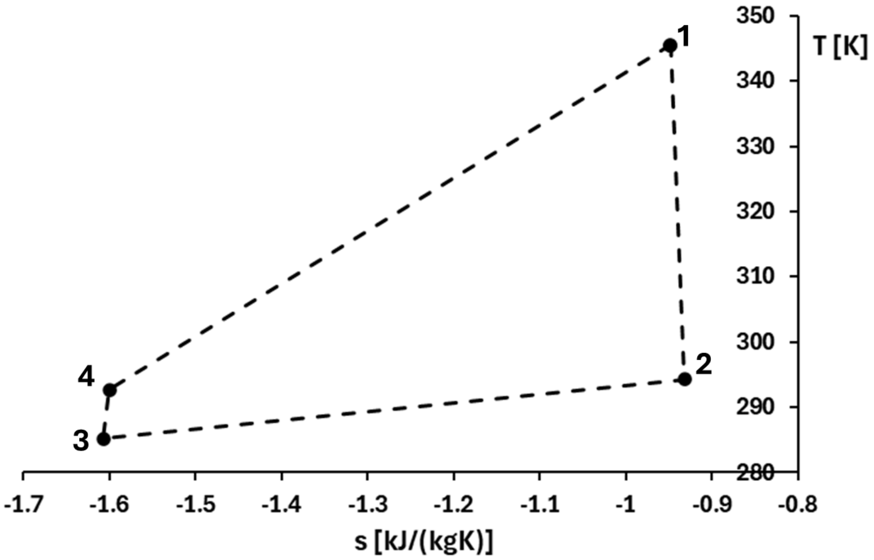

Figure 4. Thermodynamic cycle of the geothermal power plant in T-s chart.

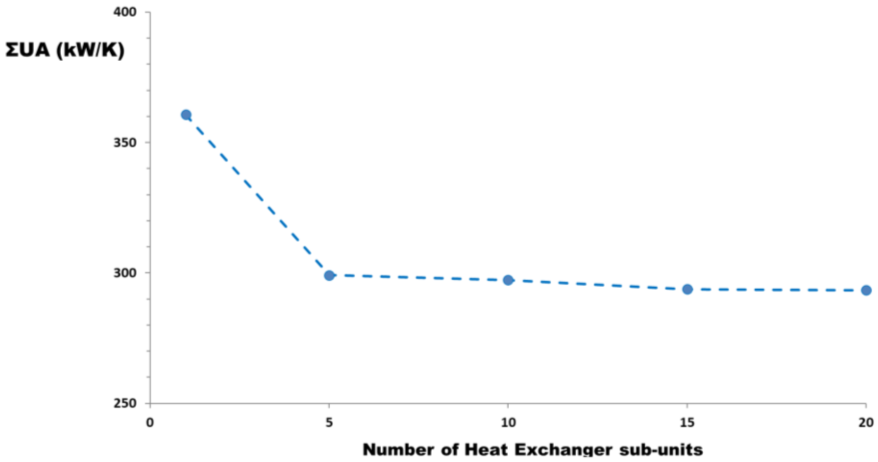

Figure 5. UA vs number of heat exchangers sub-units for geothermal heat exchanger (counterflow alignment is assumed).

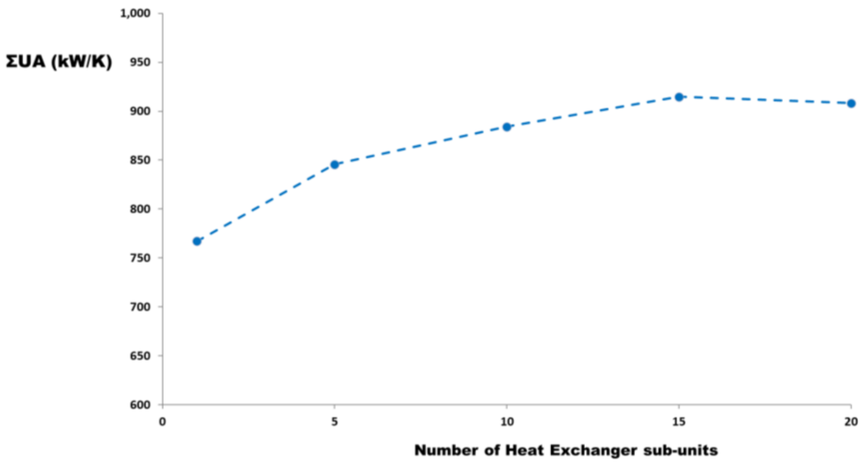

Figure 6. UA vs number of heat exchangers sub-units for condenser heat exchanger (counterflow alignment is assumed).

In the subsequent step, based on the thermodynamic cycle results and the estimated UA values of the heat exchangers, the purchase costs of the main components of the geothermal power plant were evaluated using the dedicated correlations from the international literature, as presented in **Table 3**. The results are illustrated in **Figure 7**, which presents the percentage distribution of the cost-components.

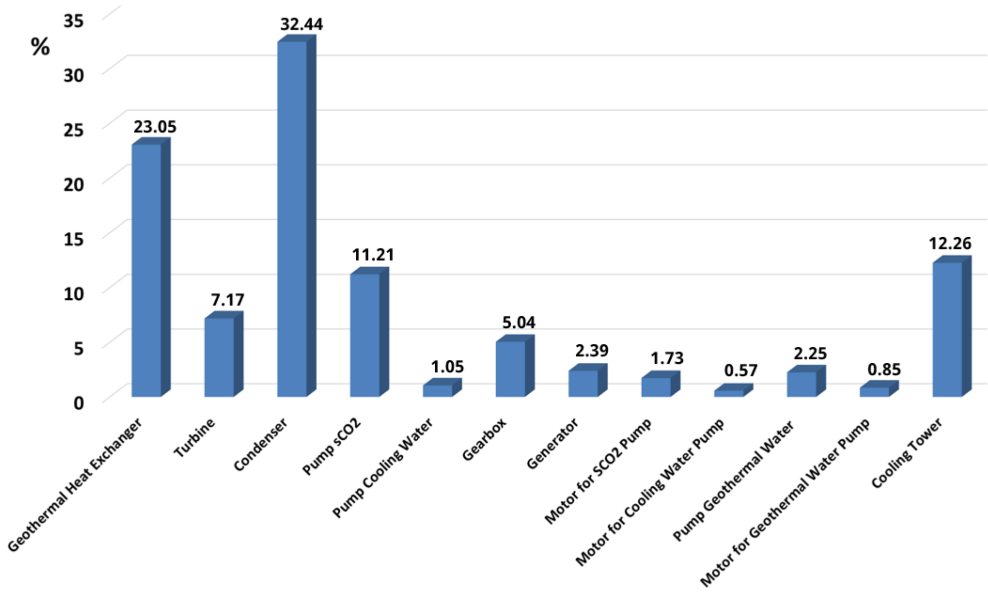

Figure 7. Percentage distribution of the cost – components.

Additionally, to evaluate the performance of the geothermal power plant under varying condensation temperatures and alternative working fluids, such as R134a, supplementary simulations were performed using the open-source DWSIM software [39], which incorporates the CoolProp library for calculating the thermophysical properties of R134a. The results, presented in **Figure 8**, correspond to maximum temperature conditions similar to the ones applied of the Sidirokastro geothermal field, taking also into account the conclusions from the works of Karypidis et al. [27] for sCO_2, and Aneke et al. [15] for R134a. A more detailed comparison of the performance of the low enthalpy geothermal field power plant of Chena, Alaska corresponding to the specific conditions described in Aneke et al. [15], carried out using Coolprop free properties library is presented in **Table 5**, where the presented results are compared to the ones of Aneke et al. [15] which were carried out with the commercial Simulation Software SimTech IPSEpro [40]. The total process that was followed in the analyses in this work is presented in **Figure 9**.

Table 5. **Components cost percentage distribution net values.**

Component	CoolProp	Difference in relation to Aneke et al. [14]	Unit
Geothermal Heat Exchanger	2571.36	0.12	kW
Turbine	265.60	0.2	kW
Condenser	2328.02	-0.02	kW
Pump sCO_2	22.27	0.05	kW
Thermal efficiency	9.463	0.005	%

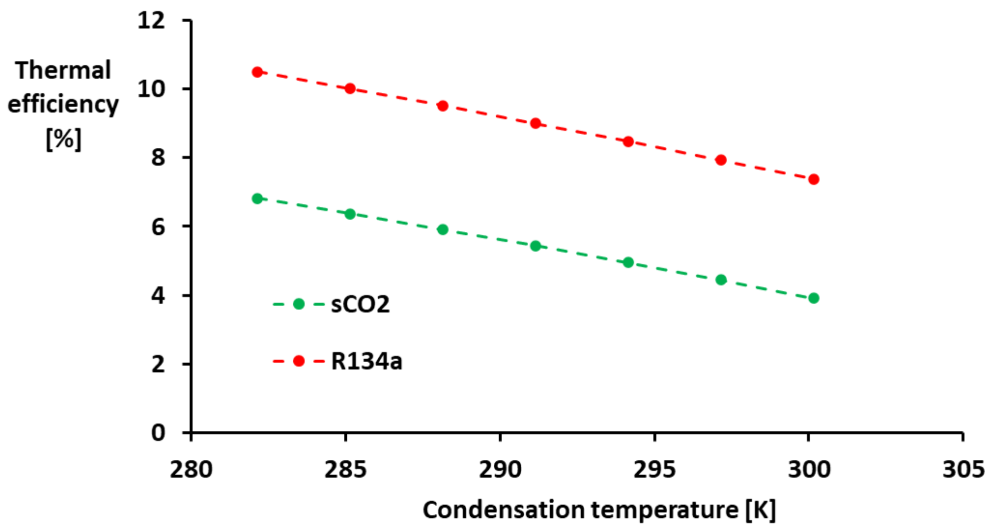

Figure 8. Thermal efficiency variation vs condensation temperature for sCO_2 and R134a.

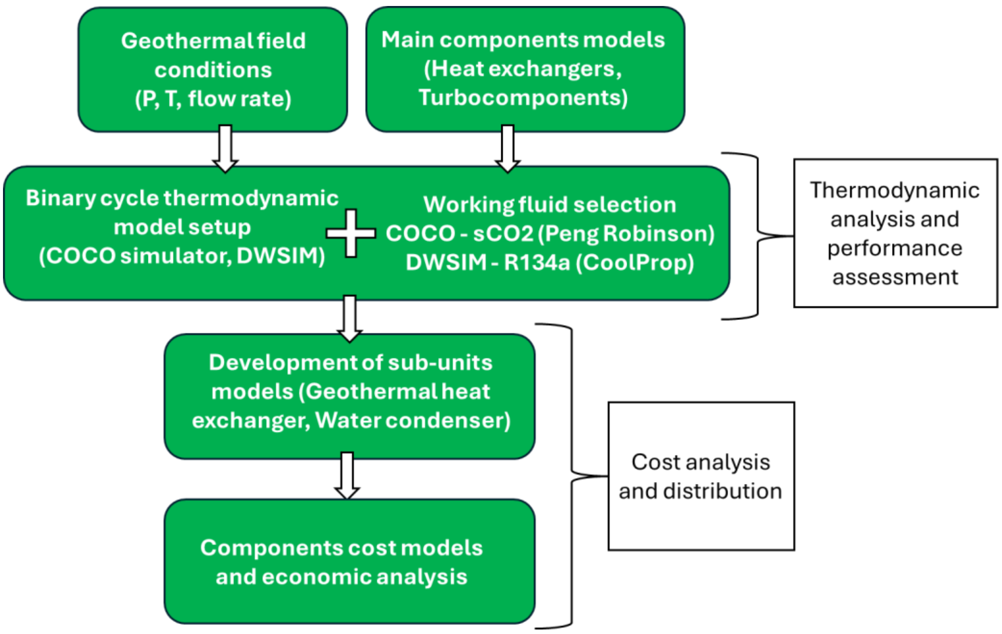

Figure 9. Analysis flow chart.

4. Discussion and Conclusions

In the present study a thermodynamic model was developed in COCO simulator to represent the conditions of the low enthalpy geothermal field located in the region of Sidirokastro near the city of Serres, Greece, incorporating the most recent available data on the geothermal source properties. In the thermodynamic model, the performance characteristics of the geothermal power plant components were defined using benchmark data from the international literature on comparable applications. According to these results, a preliminary analysis of the geothermal power plant efficiency and cost-components distribution was performed. More specifically, as can be seen in **Table 4**, the performance of the geothermal power plant is characterized by a relatively low thermal efficiency value of 5.46%. This value can be mainly attributed to the combination of (a) relatively low geothermal source temperature, i.e., 78 °C, (b) low turbine pressure ratio, i.e., ~1.925, as a result of the condensation temperature value and (c) relatively high sCO_2 pump consumption. As a result, the geothermal power plant produces ~250 kW since a large part of the turbine generated power of ~425 kW is consumed for the operation of the sCO_2 pump, which requires ~175 kW.

Regarding component costs, which were estimated using the most recent correlations from the international literature, the water condenser and the geothermal heat exchanger were identified as the most cost-intensive elements, together accounting for over 55% of the total equipment purchase cost. the water condenser represents the highest share, accounting for 32.44% of the total power plant component purchase cost, while the geothermal heat exchanger follows as the second most expensive component, corresponding to 23.05% of the total. The cost of the cooling tower, the sCO_2 pump, the sCO_2 turbine and the gearbox cost are also significant corresponding to 12.26%, 11.21%, 7.17% and 5.04% respectively. Finally, the cost of the generator, motors and the water pumps are considerably lower ranging from 2.39% to 0.57%.

For the estimation of the heat exchangers costs, i.e. the water condenser and the geothermal heat exchanger costs, which depend on the UA parameter (the product of the overall heat transfer coefficient and the heat exchanger surface area), detailed sub-models were employed to accurately capture the influence of CO_2 thermophysical property variations on the calculation of the logarithmic mean temperature difference (LMTD) and, consequently, on the UA value. In the cost calculations, the final UA values corresponding to the 20 sub-units configuration, as presented in **Figure 5** and **Figure 6**, were used as the most accurate values. These values are considered stabilized beyond 15 sub-units, showing only about 0.1% and 0.7% deviation for the geothermal heat exchanger and the water condenser, respectively, compared to the 15 sub-units results.

In comparison with one of the most well-documented low-enthalpy geothermal applications in the international literature—the Chena, Alaska power plant using R134a as the working fluid, described by Aneke et al. [15] and Holdmann [41]—the performance of the Sidirokastro low-enthalpy geothermal power plant using sCO_2 is approximately 4% lower in terms of net thermal efficiency. However, the components purchase total cost is more than 40% higher, based on the best available data reported by Holdmann [41] which indicate total project expenses of $2,007,770 by the end of 2006. The cost comparison was performed by adjusting all component costs to 2017 USD values using the Chemical Engineering Plant Cost Index (CEPCI), as reported by Weiland et al. [33], where the CEPCI 2017 index was 567.5.

However, it should be mentioned that a part of this cost difference can be attributed to the fact that the Chena, Alaska power plant operates with a combination of water condenser and air cooler. Owing to Alaska’s low ambient temperatures, the use of an air cooler can be thermodynamically efficient during certain periods, resulting in an approximately 10% reduction in net cost compared to systems utilizing only a water condenser. Furthermore, the use of R134a in the Chena, Alaska power plant facilitates the use of commercially widely available components and heat exchangers, as mentioned in Holdmann

[41], resulting in lower cost in relation to sCO_2, for which the technological maturity has not yet reached the same level.

As can be seen also in **Figure 8**, in all cases the use of R134a results in improved thermodynamic cycle performance in relation to sCO_2. However, taking into consideration the planned hydrofluorocarbon (HFC) phase-down in Europe for 2030 the use of carbon dioxide as working fluid becomes more interesting. Thus, further efforts are required to enhance the performance of sCO_2-based thermodynamic cycles, given the significant environmental advantages associated with replacing HFCs with carbon dioxide.

It is also important to note that future studies should incorporate more detail and up-to-date data in component cost correlations and extend these correlations to a broader range of power outputs (<1 MW), while also considering the latest technological developments and advancements in the field. In addition, detailed thermoeconomic models for the heat exchangers should be developed, in order to correlate the heat exchangers design geometrical and performance characteristics to the achieved thermal effectiveness and imposed pressure drop and thus, to the effect on the binary cycle thermodynamic efficiency. Furthermore, material selection and manufacturing limitations should also be taken into consideration to the heat exchangers purchase cost and the binary cycle power plant economic performance. These actions will increase the cost correlations range of validity, reduce the analysis uncertainty degree, and provide a significant design tool for the optimization of the power plant, whilst also taking into account both thermodynamic and cost-related technoeconomic parameters. Last but not least, future efforts will focus on the evaluation of the thermodynamic and technoeconomic performance of the low-enthalpy geothermal field combined with supplementary renewable energy sources (mainly solar energy). This will allow to increase the temperature of the sCO_2 before the latter enters the turbine, thereby enhancing the power generation potential and the cycle's thermal efficiency, providing a more cost-effective and environmentally friendly solution.

The present work is a follow-up analysis of previous works concerning the low enthalpy geothermal field located in the region of Sidirokastro in Serres, Greece, this time focusing on a detailed analysis of the binary cycle components cost, which was not so far included. To the authors' best available information and knowledge this is the first time such an analysis has been presented for low enthalpy geothermal applications specifically refering to Greece's geothermal fields. Key aspects differentiating the present work in relation to most existing literature works are: (a) the use of supercritical carbon dioxide as working fluid combined with the use of a low enthalpy heat source in a binary cycle, (b) the use of only open source and free software for the modelling approaches and (c) the development of detailed heat exchangers models specifically targeting the accurate calculation of UA values taking into account the working fluid thermophysical properties variation during the heat transfer process.

It worths also to mention that targeting the efficiency improvement of power plants and energy systems, special interest has been presented in international literature on hybrid systems utilizing recuperative and regenerative cycles [42] and power plants combining more than one heat sources, more notably solar and geothermal energy sources, as presented in [43,44]. All these combinations can present enhanced opportunities for more efficient utilization of energy sources as opposed to standalone systems and power plants, especially when low enthalpy geothermal sources are considered as the prime energy source, and thus, are planned to be strongly considered in the near future for low enthalpy geothermal applications as the one presented in this work.

Abbreviations

The following abbreviations are used in this manuscript:

ω	A dimensionless parameter specific to each chemical species that influences its vapor-pressure behavior.
P_c	Critical Pressure
T_c	Critical Temperature
R	The ideal gas constant R=8.314413 J/mol*K
GHG	GreenHouse Gas
GWP	Global Warming Potential
ODP	Ozone Depletion Potential
ORC	Organic Rankine Cycles
sCO_2	Supercritical Carbon Dioxide
HEX	Heat Exchanger
HFC	Hydrofluorocarbon

Declarations

Ethics Statement

Not applicable

Consent for Publication

Not applicable

Availability of Data and Material

Dataset available on request from the authors.

Funding

No financial support has been received for the work presented in this paper.

Competing Interests

The authors have declared that no competing interests exist.

Author Contributions

Conceptualization: D.M., C.P. and A.K.; Methodology: A.K. and D.M. (Thermodynamics), C.P. and K.K. (Cost analysis); Software: A.K., D.M.; Validation: All; Formal Analysis: All; Investigation: All.; Writing – Original Draft: A.K., D.M., C.P.; Writing – Review & Editing: All; Visualization: All; Supervision: D.M., C.P.

References

1. European Commission. A European Green Deal: Striving to be the First Climate-Neutral Continent [Internet]. 2022 [cited 2025 Apr 24]. Available from: https:commission.europa.eu/strategy-and-policy/priorities-2019-2024/european-green-deal_en.
2. Ismail B. Introductory Chapter: Power Generation Using Geothermal Low-Enthalpy Resources and ORC Technology [Internet]. Renewable Geothermal Energy Explorations. IntechOpen; 2019 April 03 [cited 2025 October 22]. Available from: http://dx.doi.org/10.5772/intechopen.84390.
3. Eliasson ET, Thorhallsson S, Steingrimsson B. GEOTHERMAL POWER PLANTS. Geothermal Project Management and Development, 2008; Short Course on Geothermal Project Management and Development, organized by UNU-GTP, KenGen and MEMD-DGSM. Entebbe, Uganda. November 20-22, 2008.
4. Sigfusson B, Uihlein A. Joint Research Centre, Institute for Energy and Transport, 2014 JRC Geothermal Energy Status Report: Technology, market and economic aspects of geothermal energy in Europe. Luxembourg: Publications Office of the European Union, 2015. Report No.: JRC93338. Available from: https://data.europa.eu/doi/10.2790/460251.
5. Ismail BI. Advanced electrical power generation technology using renewable & clean low-enthalpy geothermal energy sources. Recent Pat Mech Eng. 2011;4(2):168-179. DOI
6. Lipan LC, Dimitriu S, Florea GA. Smart Combined Heat and Power System, Using Geothermal Low Enthalpy Resources [Internet]. Smart Cities - Foundations and Perspectives. IntechOpen; 2024 April 2 [cited 2025 October 22]. Available from: http://dx.doi.org/10.5772/intechopen.114303.
7. Ismail BI. Power Generation Using Nonconventional Renewable Geothermal & Alternative Clean Energy Technologies [Internet]. Planet Earth 2011 - Global Warming Challenges and Opportunities for Policy and Practice. InTech; 2011 October 3 [cited 2025 October 22]. Available from: http://dx.doi.org/10.5772/25132.
8. Morrone P, Algieri A, Castiglione T. Hybridisation of biomass and concentrated solar power systems in transcritical organic Rankine cycles: A micro combined heat and power application. Energy Convers Manag. 2019;180:757-768. DOI
9. Eyerer S, Dawo F, Wieland C, Spliethо, H. Advanced ORC architecture for geothermal combined heat and power generation. Energy. 2020;205:117967. DOI
10. Yaduvanshi A. Geothermal Turbines Market Size & Outlook, 2025-2033. Geothermal Turbines Market Size, Share & Trends Analysis Report By Type (Dry Steam, Flash Cycle, Binary Cycle), By Application (Industrial, Residential, Agricultural, Others) and By Region (North America, Europe, APAC, Middle East and Africa, LATAM) Forecasts, 2025-2033 [Internet]. 2025 January [cited 2025 October 22]. Report Code: SREP55670DR. Available from: https://straitsresearch.com/report/geothermal-turbines-market.
11. Lee J-Y, Chen S-L. Optimal Design of a Geothermal Organic Rankine Cycle System. Chem Eng Trans. 2022;94:523-528. DOI
12. Morrone P, Algieri A. Integrated Geothermal Energy Systems for Small-Scale Combined Heat and Power Production: Energy and Economic Investigation. Appl Sci. 2020;10(19):6639. DOI
13. Bianchi M, Branchini L, De Pascale A, Melino F, Ottaviano S, Peretto A, et al. Performance and operation of micro-ORC energy system using geothermal heat source. Energy Procedia. 2018;148:384-391. DOI
14. Calise F, Cappiello FL, Dentice d'Accadia M, Vicidomini M. Thermo-Economic Analysis of Hybrid Solar-Geothermal Polygeneration Plants in Different Configurations. Energies. 2020;13(9):2391. DOI
15. Aneke M, Agnew B, Underwood C. Performance analysis of the Chena binary geothermal power plant. Appl Therm Eng. 2011;31:1825-1832. DOI
16. Karytsas C, Kontoleontos E, Mendrinos D. Project LOW-BIN Efficient Low Temperature Geothermal Binary Power. Proceedings of European Geothermal Congress 2007. 2007 May 30-June 1; Unterhaching, Germany.
17. Andritsos N, Arvanitis A, Papachristou M, Fytikas M, Dalambakis P. Geothermal activities in Greece during 2005-2009. Proceedings of the World Geothermal Congress 2010. 2021 Apr 25-30; Bali, Indonesia.

18. Andritsos N, Dalambakis P, Arvanitis A, Papachristou M, Fytikas M. Geothermal developments in Greece – Country update 2010-2014. Proceedings of World Geothermal Congress. 2015 Apr 16-24. Melbourne, Australia.
19. Thurairaja K, Wijewardane A, Jayasekara S, Ranasinghe C. Working Fluid Selection and Performance Evaluation of ORC. Energy Procedia. 2019;156,244-248. DOI
20. European Environment Agency (EEA). Hydrofluorocarbon phase-down in Europe [Internet]. 2025 [cited 2025 June 5]. Available from: https://www.eea.europa.eu/en/analysis/indicators/hydrofluorocarbon-phase-down-in-europe.
21. EAGME started a second drilling in the Sidirokastro geothermal field, Serres [Internet]. 2022 May 25 [cited 2026 January 3]. Available from: https://eagme.gr/pages/h-eagme-ksekinhse-kai-deyterh-gewtrhsh-sto-gewthermiko-pedio-sidhrokas (in Greek).
22. Calm J, Hourahan G. Physical, Safety, and Environmental Data for Current and Alternative Refrigerants. Proceedings of the 23rd International Congress of Refrigeration. 2011 August 21–26; Prague, Czech Republic.
23. Saleh B. Parametric and working fluid analysis of a combined organic Rankine-vapor compression refrigeration system activated by low-grade thermal energy. J Adv Res. 2016;7(5):651-660. DOI
24. ASHRAE. ANSI/ASHRAE Addendum f to ANSI/ASHRAE Standard 34-2019. Designation and Safety Classification of Refrigerants [Internet]. 2019 October 16 [cited 2025 October 22]. Available from: https://www.ashrae.org/file%20library/technical%20resources/standards%20and%20guidelines/standards%20addenda/34_2019_f_20191213.pdf.
25. Chen Y. Thermodynamic cycles using carbon dioxide as working fluid - CO2 transcritical power cycle study [dissertation]. Stockholm, Sweden: KTH; 2011.
26. COCO. The CAPE-OPEN simulator [software]. COCO version 3.5. 2024 April [cited 2025 April 07]. Available from: www.cocosimulator.org/index.html.
27. Karypidis AI, Misirlis D, Chasapis D, Papadopoulos PA, Moissiadis A, Kleidis K. Preliminary thermodynamic analysis of the performance of a low enthalpy geothermal field in the region of sidirokastron in serres. Proceedings of the 13^{th} National Conference for Soft Energy Applications. 2024 May 15-17; Athens, Greece.
28. Tangsriwong K, Lapchit P, Kittijungjit T, Klamrassamee T, Sukjai Y, Laoonual Y. Modeling of chemical using commercial processes and open-source software: A comparison between Aspen Plus and DWSIM. IOP Conf Ser: Earth Environ Sci. 2020;463:012057. DOI
29. Peng DY, Robinson DB. A New Two-Constant Equation of State. Ind Eng Chem Fundam. 1976;15,59–64. DOI
30. Atinga KA. Simulation Modelling and Techno-Economics of Supercritical Carbon Dioxide Recompression Closed Brayton Cycle. EPE. 2024;16,325-344. DOI
31. Crespi F, de Arriba PR, Sánchez D, Muñoz A. Preliminary investigation on the adoption of CO_2-SO_2 working mixtures in a transcritical Recompression cycle. Appl Therm Eng. 2022;211:118384. DOI
32. Siddiqui ME, Almitani KH. Proposal and Thermodynamic Assessment of S-CO_2 Brayton Cycle Layout for Improved Heat Recovery. Entropy. 2020; 22(3):305. DOI
33. Weiland NT, Lance BW, Pidaparti SR. sCO2 Power Cycle Component Cost Correlations From DOE Data Spanning Multiple Scales and Applications. Proceedings of the ASME Turbo Expo 2019: Turbomachinery Technical Conference and Exposition. Volume 9: Oil and Gas Applications; Supercritical CO2 Power Cycles; Wind Energy. 2019 June 17-21; Phoenix, Arizona, USA. DOI
34. Carlson MD, Middleton BM, Ho CK. Techno-Economic Comparison of Solar-Driven sCO2 Brayton Cycles using Component Cost Models Baselined with Vendor Data and Estimates. Proceedings of the ASME 2017 11th International Conference on Energy Sustainability collocated with the ASME 2017 Power Conference Joint With ICOPE-17, the ASME 2017 15th International Conference on Fuel Cell Science, Engineering and Technology, and the ASME 2017 Nuclear Forum. ASME 2017 11th International Conference on Energy Sustainability. 2017 June 26–30; Charlotte, North Carolina, USA. DOI
35. McCollum DL, Ogden JM. Techno-Economic Models for Carbon Dioxide Compression, Transport, and Storage & Correlations for Estimating Carbon Dioxide Density and Viscosity [dissertation]. Davis, USA: Institute of Transportation Studies, University of California; 2006.

36. Towler, G. Sinnott, R. Chemical Engineering Design. Principles, Practice and Economics of Plant and Process Design. 3rd ed. Oxford, UK: Elsevier; 2021.
37. Arbula Blecich A, Blecich P. Thermoeconomic Analysis of Subcritical and Supercritical Isobutane Cycles for Geothermal Power Generation. Sustainability. 2023;15(11):8624. DOI
38. Shamoushaki M, Niknam PH, Talluri L, Manfrida G, Fiaschi D. Development of Cost Correlations for the Economic Assessment of Power Plant Equipment. Energies. 2021; 14(9):2665. DOI
39. DWSIM. The Open Source Chemical Process Simulator [software]. DWSIM, 2025 [cited 2025 Apr 20]. Available from: dwsim.org/.
40. SimTech. IPSEpro PSE version 4.0 [software]. SimTech Simulation Technology, 2008 [cited 2025 Jun 4]. Available from: www.simtechnology.com.
41. Holdmann G. The Chena Hot Springs 400 kW Geothermal Power Plant: Experience Gained During the First Year of Operation. GRC Transactions. 2007;31:515-519.
42. Jiménez-García JC, Ruiz A, Pacheco-Reyes A, Rivera W. A Comprehensive Review of Organic Rankine Cycles. Processes. 2023;11(7):1982. DOI
43. Song J, Wang Y, Wang K, Wang J, Markides CN. Combined supercritical CO2 (SCO2) cycle and organic Rankine cycle (ORC) system for hybrid solar and geothermal power generation: Thermoeconomic assessment of various configurations. Renew Energy. 2021;174:1020-1035. DOI
44. Kariuki BW, Hassan H, Ahmed M, Emam M. A review on geothermal-solar hybrid systems for power production and multigeneration systems. Appl Therm Eng. 2025;259:124796. DOI